

A frustrated quantum spin- s model on the Union Jack lattice with spins $s > \frac{1}{2}$

R.F. Bishop and P. H. Y. Li

School of Physics and Astronomy, The University of Manchester, Schuster Building, Manchester, M13 9PL, United Kingdom

Received: date / Revised version: date

Abstract. The zero-temperature phase diagrams of a two-dimensional frustrated quantum antiferromagnetic system, namely the Union Jack model, are studied using the coupled cluster method (CCM) for the two cases when the lattice spins have spin quantum number $s = 1$ and $s = \frac{3}{2}$. The system is defined on a square lattice and the spins interact via isotropic Heisenberg interactions such that all nearest-neighbour (NN) exchange bonds are present with identical strength $J_1 > 0$, and only half of the next-nearest-neighbour (NNN) exchange bonds are present with identical strength $J_2 \equiv \kappa J_1 > 0$. The bonds are arranged such that on the 2×2 unit cell they form the pattern of the Union Jack flag. Clearly, the NN bonds by themselves (viz., with $J_2 = 0$) produce an antiferromagnetic Néel-ordered phase, but as the relative strength κ of the frustrating NNN bonds is increased a phase transition occurs in the classical case ($s \rightarrow \infty$) at $\kappa_c^{\text{cl}} = 0.5$ to a canted ferrimagnetic phase. In the quantum cases considered here we also find strong evidence for a corresponding phase transition between a Néel-ordered phase and a quantum canted ferrimagnetic phase at a critical coupling $\kappa_{c_1} = 0.580 \pm 0.015$ for $s = 1$ and $\kappa_{c_1} = 0.545 \pm 0.015$ for $s = \frac{3}{2}$. In both cases the ground-state energy E and its first derivative $dE/d\kappa$ seem continuous, thus providing a typical scenario of a second-order phase transition at $\kappa = \kappa_{c_1}$, although the order parameter for the transition (viz., the average ground-state on-site magnetization) does not go to zero there on either side of the transition.

PACS. 75.10.Jm Quantized spin models – 75.30.Kz Magnetic phase boundaries – 75.50.Ee Antiferromagnetics – 75.50.Gg Ferrimagnetics

1 Introduction

In a recent paper [1] we have used the coupled cluster method (CCM) [2,3,4] to study the magnetic order on a frustrated Heisenberg antiferromagnetic system defined on the Union Jack lattice described in Sec. 2 below. In the earlier paper [1] we studied the case of particles with spin quantum number $s = \frac{1}{2}$. In the present paper we further the investigation of this frustrated Union Jack model by replacing the spin- $\frac{1}{2}$ particles with particles with higher values of s . In particular we study each of the cases $s = 1$ and $s = \frac{3}{2}$, both of which are computationally more challenging than the previous case with $s = \frac{1}{2}$. Just as in the earlier paper, however, we again use the much-studied CCM. Our main rationale for the present work is that one knows in broad terms that the value of the spin quantum number s can play an important and often highly non-trivial role in the behaviour of strongly correlated magnetic-lattice systems. They often exhibit rich and interesting phase structures that are themselves a consequence of the interplay between the quantum fluctuations and the frustration due to the competing interactions present in the system under study. The strength of

the quantum fluctuations can itself be tuned, for example, either by introducing anisotropy terms in the Hamiltonian (and see Refs. [5,6,7] for examples) or by varying the value of the spin quantum number s of the particles (and see Ref. [8] for an example). In the present paper we study the effect on the Union Jack model of increasing s , in order to throw more light on the mechanisms for magnetic ordering inherent in the system. Alternative ways of varying the quantum fluctuations, not studied here, would be to introduce anisotropy into one or both of the magnetic Heisenberg bonds present, either in real space (and see Ref. [7] for an example) or in spin space (and see Refs [6,8] for example).

The general field of quantum magnetism at zero temperature, for spins on the sites of regular lattices in two spatial dimensions [9,10,11], has become an important and fascinating subject in recent years, and one that is at the forefront of modern condensed matter research. Much attention has been focussed on frustrated systems where different types of bonds are in competition with one another, especially when each type acting alone produces a different ground-state (gs) ordering and a different phase. A set of touchstone problems in this respect is the case of the two-dimensional (2D) square-lattice Heisen-

Send offprint requests to:

berg antiferromagnet (HAF) with nearest-neighbour (NN) exchange bonds with strength $J_1 > 0$ that by themselves produce a Néel-ordered phase, but now with the addition of frustrating next-nearest-neighbour (NNN) bonds of strength $J_2 > 0$ on some or all of the diagonals of some or all of the fundamental square-lattice plaquettes. A review of the “pure” system for $J_2 = 0$ is given in Ref. [12]. Although quantum fluctuations certainly act to destroy the perfect Néel antiferromagnetic ordering of the classical model (equivalent to the limiting case $s \rightarrow \infty$), it is well established that for the $s = \frac{1}{2}$ case the order parameter, namely the sublattice or staggered magnetization, has a value equal to about 61% of the classical limiting value. For such unfrustrated 2D models the most accurate results are generally provided by quantum Monte Carlo (QMC) simulations (and see, e.g., Ref. [13] for the spin-half HAF on the 2D square lattice).

Once NNN bonds are added to the above pure spin- $\frac{1}{2}$ HAF the situation becomes much more complicated. The prototypical model in this respect is the so-called J_1 - J_2 model in which all possible NNN bonds are included, and which finds good experimental realization in such layered materials as $\text{Li}_2\text{VO}_2\text{SiO}_4$, $\text{BaCdVO}(\text{PO}_4)_2$, and others. Various approximate methods have been used to simulate the properties of this system, including the coupled cluster method (CCM) [6, 7, 14, 15, 16], series expansion (SE) techniques [17, 18, 19, 20, 21], exact diagonalization (ED) methods [22, 23, 24], and hierarchical mean-field (MF) calculations [25]. For frustrated spin-lattice models in two dimensions both the QMC and ED techniques face formidable difficulties. These arise in the former case due to the “minus-sign problem” present for frustrated systems when the nodal structure of the gs wave function is unknown, and in the latter case due to the practical restriction to relatively small lattices imposed by computational limits. The latter problem is exacerbated for incommensurate phases, and is compounded due to the large (and essentially uncontrolled) variation of the results with respect to the different possible shapes of clusters of a given size.

Several other models of this same general class of spin- $\frac{1}{2}$ models on the 2D square lattice with both NN and NNN interactions present, but in which some of the NNN J_2 bonds are removed, have prompted considerable recent interest. One such is the Shastry-Sunderland model [26, 27, 28], in which three-quarters of the J_2 bonds of the J_1 - J_2 model are removed in a particular arrangement so that each lattice site is connected by four NN J_1 bonds and one NNN J_2 bond. The Shastry-Sunderland model finds a good experimental realization in the magnetic material $\text{SrCu}(\text{BO}_3)_2$. A second such model, in which half of the J_2 bonds of the J_1 - J_2 model are removed in an arrangement that leaves each lattice site connected by four NN J_1 bonds and two NNN J_2 bonds, is the anisotropic triangular lattice (or J_1 - J'_2) model [29], which is also believed to well describe the layered magnetic material Cs_2CuCl_4 . A third such model, in which again half of the J_2 bonds of the J_1 - J_2 model are removed, but now in an arrangement that leaves half of the sites eight-connected (namely,

by four NN J_1 bonds and four NNN J_2 bonds) and the other half four-connected by J_1 bonds alone, is the Union Jack model [1, 30, 31, 32], whose study we continue here by extending the situation to where the spins have spin quantum number $s > \frac{1}{2}$. Although all of the models mentioned above show antiferromagnetic Néel ordering for small values of J_2 , their phase diagrams for larger values of J_2 display a wide variety of behaviour, including, two-dimensional quantum “spirals”, valence-bond crystals/solids, and spin liquids [33]. Thus, in the absence of any definitive overarching theoretical argument, the best way to understand this class of NN/NNN models on the square lattice is to treat each one on a case-by-case basis.

While the general trend is that as the spin quantum number s is increased the effects of quantum fluctuations reduce, one also knows that there can be significant deviations from it. A particularly well-known example is the since-confirmed prediction of Haldane that integer-spin systems on the linear chain would have a nonzero excitation energy gap, whereas half-odd-integer spin systems would be gapless [34]. Indeed, such deviations from general trends provide one of the main reasons why quantum spin-lattice problems still maintain such an important role in the general investigation of quantum phase transitions.

For the past few decades, a great deal of attention has also been devoted to magnetic materials with spin-1 ions (see, e.g., Refs. [35] and references cited therein). In this context we note the recent discovery of superconductivity with a transition temperature at $T_c \approx 26$ K in the layered iron-based compound LaOFeAs , when doped by partial substitution of the oxygen atoms by fluorine atoms [36], $\text{La}[\text{O}_{1-x}\text{F}_x]\text{FeAs}$, with $x \approx 0.05$ – 0.11 . This has been followed by the rapid discovery of superconductivity at even higher values of T_c ($\gtrsim 50$ K) in a broad class of similar doped quaternary oxypnictide compounds. Enormous interest has thereby been engendered in this class of materials. Of particular relevance to the present work are the very recent first-principles calculations [37] showing that the undoped parent precursor material LaOFeAs is well described by the spin-1 J_1 - J_2 model on the square lattice with $J_1 > 0$, $J_2 > 0$, and $J_2/J_1 \approx 2$. Broadly similar conclusions have also been reached by other authors [38]. It is clear, therefore, that the theoretical study of 2D quantum magnets with $s = 1$ (or $s > 1$) are worthy of pursuit in their own right, as well as to highlight differences with their $s = \frac{1}{2}$ counterpart.

In this article we continue the study, begun in Ref. [1] for the $s = \frac{1}{2}$ case, of magnetic ordering in the Union Jack model, by now extending the discussion to the two cases where the spins have either $s = 1$ or $s = \frac{3}{2}$. The model itself is discussed in more detail in Sec. 2 below. For the $s = \frac{1}{2}$ case the model has been studied previously using SWT [30, 31] and SE techniques [32], as well as by the CCM [1] used here. However, to our knowledge, no results have yet been reported for the cases with $s > \frac{1}{2}$.

As in the case of the spin-half anisotropic triangular lattice (or J_1 - J'_2) model, it was shown [30, 31, 32] that NN Néel order for the $s = \frac{1}{2}$ Union Jack model persists until a critical value of the frustrating NNN (J_2) bonds. However,

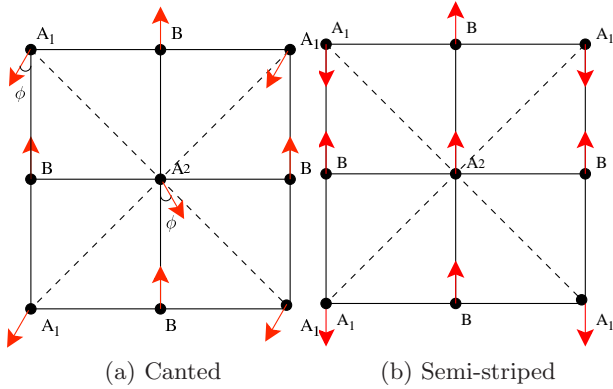


Fig. 1: Union Jack model; — J_1 ; - - - J_2 . (a) Canted state; (b) semi-stripped state. The unit cell is a square of side length 2.

in contrast to the case of the anisotropic triangular lattice model, there exists a ferrimagnetic ground state in which spins on the eight-connected sites cant at a nonzero angle with respect to their directions in the corresponding Néel state. This model thus exhibits an overall magnetic moment in this regime, which is quite unusual for spin- $\frac{1}{2}$ 2D materials with only Heisenberg bonds and which therefore preserve (spin) rotational symmetries in the Hamiltonian. This model also presents us with a difficult computational task in order to simulate its properties. Here we wish to continue to study this model for the $s = 1$ and $s = 3/2$ cases using the CCM, which has consistently been shown to yield insight into a wide range of problems in quantum magnetism.

2 The model

The Hamiltonian of the Union Jack model considered here is given by

$$H = J_1 \sum_{\langle i,j \rangle} \mathbf{s}_i \cdot \mathbf{s}_j + J_2 \sum_{[i,k]} \mathbf{s}_i \cdot \mathbf{s}_k, \quad (1)$$

where the operators $\mathbf{s}_i \equiv (s_i^x, s_i^y, s_i^z)$ are the quantum spin operators on lattice site i with $\mathbf{s}_i^2 = s(s+1)$ where, for the cases considered here, $s = 1, \frac{3}{2}$. On the underlying 2D square lattice the sum over $\langle i, j \rangle$ runs over all distinct NN bonds with strength J_1 , while the sum over $[i, k]$ runs over only half of the distinct NNN diagonal bonds having strength J_2 and with only one diagonal bond on each square plaquette as arranged in the pattern shown explicitly in Fig. 1. The unit cell is thus the 2×2 square shown in Fig. 1. (We note that, by contrast, the J_1 - J_2 model discussed above includes all of the diagonal NNN bonds on the square lattice, and its unit cell is thus the 1×1 square.) We again consider the case where both sorts of bonds are antiferromagnetic, $J_1 > 0$ and $J_2 \equiv \kappa J_1 > 0$, and thus act to compete against (or to frustrate) each

other. Henceforth we set $J_1 \equiv 1$. We consider the model equivalently defined by the Union Jack geometry in which there are two sorts of sites, namely the A sites with eight NN sites and the B sites with four NN sites, as shown in Fig. 1(a).

Considered as a classical model, (and thus corresponding to the quantum case in the limit where the spin quantum number $s \rightarrow \infty$), the Union Jack model has only two ground-state (gs) phases as the parameter κ is varied over the range $(0, \infty)$. A simple variational analysis for the classical model reveals that for $0 < \kappa < \frac{1}{2}$ the gs phase is Néel-ordered, exactly as for the full J_1 - J_2 model. The Néel ordering induced by the J_1 bonds acting alone is hence preserved as the strength of the competing J_2 bonds is increased, until the critical value $\kappa_c^{\text{cl}} = 0.5$ is reached. For $\kappa > \kappa_c^{\text{cl}}$ a new phase of lower energy emerges, just as in the full J_1 - J_2 model. For the full J_1 - J_2 model that new phase is a classical striped state in which alternate rows (or columns) of spins are arranged antiparallel to one another, whereas the new classical gs phase for the Union Jack model is the canted ferrimagnetic state shown in Fig. 1(a). In the canted state the spins on each of the alternating A_1 and A_2 sites of the A-sublattice are canted respectively at angles $(\pi \mp \phi)$ with respect to those on the B sublattice, all of the latter of which point in the same direction. On the A sublattice each site A_1 has four NN sites A_2 , and vice versa. The angle between the NN spins on the A sublattice is thus 2ϕ .

The energy of the above canted state for the classical model is thus

$$E = Ns^2(\kappa \cos 2\phi - 2 \cos \phi), \quad (2)$$

where $J_1 \equiv 1$ and $N \rightarrow \infty$ is the number of sites. The energy is thus extremized when

$$\sin \phi(1 - 2\kappa \cos \phi) = 0. \quad (3)$$

When $\kappa < \kappa_c^{\text{cl}} \equiv 0.5$, the lowest energy corresponds to $\sin \phi = 0$ and hence to the Néel state. By contrast, when $\kappa > \kappa_c^{\text{cl}} \equiv 0.5$ the lowest energy solution is the canted state with

$$\phi_{\text{cl}} = \cos^{-1} \left(\frac{1}{2\kappa} \right). \quad (4)$$

Thus the classical gs energy is given by

$$E^{\text{cl}} = \begin{cases} Ns^2(\kappa - 2); & \kappa < \kappa_c^{\text{cl}} \equiv 0.5 \\ Ns^2 \left(-\frac{1}{2\kappa} - \kappa \right); & \kappa > \kappa_c^{\text{cl}} \equiv 0.5 \end{cases} \quad (5)$$

The classical phase transition at $\kappa = \kappa_c^{\text{cl}} \equiv 0.5$ is of continuous (second-order) type with the gs energy and its first derivative with respect to κ both continuous functions of κ , although there are finite discontinuities in the second- and higher-order derivatives at $\kappa = \kappa_c^{\text{cl}}$.

The total magnetization per site in the canted phase for the classical model is $m^{\text{cl}} = \frac{1}{2}s[1 - (2\kappa)^{-1}]$, and the model thus exhibits ferrimagnetism in this phase. Whereas ferrimagnetism more commonly occurs when the individual ionic spins have different magnitudes on different sublattices, it arises here in a case where when the spins all

have the same magnitude and all the interactions are antiferromagnetic in nature, but the frustration between them acts to produce an overall magnetization. The total magnetization m vanishes linearly as $\kappa \rightarrow \kappa_c^{\text{cl}}$ from the canted phase and then remains zero in the Néel phase for $\kappa < \kappa_c^{\text{cl}}$. The spontaneous breaking of the spin rotation symmetry is also reflected by the vanishing of the energy gap on both sides of the transition. Clearly on both sides of the transition the translation symmetry of the lattice is also broken.

As previously for the $s = \frac{1}{2}$ case [1], our aim here is to give a fully microscopic analysis of the Union Jack model for the quantum case where the spins all have spin quantum number either $s = 1$ or $s = \frac{3}{2}$. Our goal is to map out the zero-temperature ($T = 0$) phase diagrams for both cases, including the positions and orders of any quantum phase transitions that emerge. In particular we investigate the quantum analogues of the classical Néel and canted phases and calculate the effect of quantum fluctuations on the position and nature of the transition between them. We also aim to investigate, for particular regions of the control parameter κ , whether the quantum fluctuations may favour other phases, which have no classical counterparts. One such possible candidate is discussed below.

For the classical ($s \rightarrow \infty$) model the $\kappa \rightarrow \infty$ limit corresponds to a canting angle $\phi \rightarrow \frac{1}{2}\pi$, such that the spins on the A sublattice become Néel-ordered, as is expected. The spins on the antiferromagnetically-ordered A sublattice are thus orientated at 90° to those on the ferromagnetically-ordered B sublattice in this limit. In reality, of course, there is complete degeneracy at the classical level in this limit between all states for which the relative ordering directions for spins on the A and B sublattices are arbitrary. Clearly the exact $\kappa \rightarrow \infty$ limit of the Union Jack model with spins having any value of the spin quantum number s should also comprise decoupled antiferromagnetic and ferromagnetic sublattices. However, one might now expect that this degeneracy in the relative spin orientations between the two sublattices is lifted by quantum fluctuations by the well-known phenomenon of *order by disorder* [39]. Just such a phase is known to exist in the full spin- $\frac{1}{2}$ J_1 - J_2 model for values of $J_2/J_1 \gtrsim 0.6$, where it is the so-called collinear striped phase in which, on the square lattice, spins along (say) the rows in Fig. 1 order ferromagnetically while spins along the columns and diagonals order antiferromagnetically. We have also shown how such a striped state is stabilized by quantum fluctuations for values of $J'_2/J_1 \gtrsim 1.8$ for the spin- $\frac{1}{2}$ anisotropic triangular lattice model (or J_1 - J'_2 model) [29].

The existence of the striped state as a stable phase for large values of the frustration parameter for both the spin- $\frac{1}{2}$ J_1 - J_2 and J_1 - J'_2 models above is a reflection of the well-known fact that quantum fluctuations favour collinear ordering. In both cases the order-by-disorder mechanism favours the collinear state from the otherwise infinitely degenerate set of available states at the classical level. For the present Union Jack model the corresponding collinear state that might perhaps be favoured by the order by disorder mechanism is the so-called semi-striped state shown

in Fig. 1(b) where the A sublattice is now Néel-ordered in the same direction as the B sublattice is ferromagnetically ordered. Alternate rows (or columns) are thus ferromagnetically and antiferromagnetically ordered in the same direction. We investigate the possibility below that if such a semi-stripe-ordered phase may be stabilized by quantum fluctuations at larger values of κ for either of the cases $s = 1$ or $s = \frac{3}{2}$, in order to compare with the earlier $s = \frac{1}{2}$ case [1].

We note that for the $s = \frac{1}{2}$ case our own CCM calculations [1] provided strong evidence that the canted ferrimagnetic phase becomes unstable at large values of the frustration parameter κ . In view of that observation we also used the CCM for the $s = \frac{1}{2}$ case with the collinear semi-stripe-ordered ferrimagnetic state as a model state. We found tentative evidence, based on the relative energies of the two states, for a second zero-temperature phase transition between the canted and semi-stripe-ordered ferrimagnetic states at a larger critical value of $\kappa_{c_2} \approx 125 \pm 5$, as well as firm evidence for a first phase transition between the Néel antiferromagnetic phase and the canted ferrimagnetic phase at a critical coupling $\kappa_{c_1} = 0.66 \pm 0.02$. Our prediction for κ_{c_2} , however, was based on an extrapolation of the CCM results for the canted state into regimes where the solutions have already become unstable and the CCM equations based on the canted state as model state have no solutions at any level of (LSUB n) approximation beyond the lowest (with $n = 2$). The prediction for κ_{c_2} was thus less reliable than that for κ_{c_1} , although our results showed clear evidence that, if the second transition at $\kappa = \kappa_{c_2}$ does exist, it should be of first-order type. By contrast, the transition at $\kappa = \kappa_{c_1}$ for the $s = \frac{1}{2}$ case was found to be an interesting one. As in the classical ($s \rightarrow \infty$) case, the energy and its first derivative were seen to be continuous (within the errors inherent in our approximations), thus providing a typical scenario of a second-order phase transition, although a weakly first-order one could not be excluded. Nevertheless, the average on-site magnetization was seen to approach a nonzero value $M_{c_1} = 0.195 \pm 0.005$ on both sides of the transition, which is more typical of a first-order transition. The slope, $dM/d\kappa$, of the order parameter curve as a function of the coupling parameter κ , also appeared to be continuous, or very nearly so, at the critical point κ_{c_1} . Thus, all of the evidence shows that for the $s = \frac{1}{2}$ case the transition between the Néel and canted phases is a subtle one. A particular interest here is to compare and contrast the corresponding transition(s) between the $s = \frac{1}{2}$ and the $s > \frac{1}{2}$ models.

We first briefly describe the main elements of the CCM below in Sec. 3, where we also discuss the approximation schemes used in practice for the $s = \frac{1}{2}$ case and the $s > \frac{1}{2}$ cases. Then in Sec. 4 we present our CCM results based on using the Néel, canted and semi-striped states discussed above as model states (or starting states). We conclude in Sec. 5 with a discussion of the results.

3 The coupled cluster method

It is widely recognized nowadays that the CCM (see, e.g., Refs. [2,3,4] and references cited therein) employed here is one of the most powerful and most versatile modern techniques in quantum many-body theory. It has been successfully applied to various quantum magnets (see, e.g., Refs. [4,6,7,14,15,16,29,40,41,42]), and is particularly appropriate for studying frustrated systems, for which the main alternative methods are often only of limited usefulness. For example, QMC techniques are particularly plagued by the sign problem for such systems, and the ED method is often restricted in practice, particularly for $s > 1/2$, to such small lattices that it is often insensitive to the details of any subtle phase order present.

We now briefly describe the CCM means to solve the ground-state (gs) Schrödinger ket and bra equations, $H|\Psi\rangle = E|\Psi\rangle$ and $\langle\tilde{\Psi}|H = E\langle\tilde{\Psi}|$ respectively (and see Refs. [2,3,4,40,41,42] for further details). The first step in implementing the CCM is always to choose a normalized starting state or model state $|\Phi\rangle$ on top of which to incorporate later in a systematic fashion the multi-spin correlations contained in the exact ground states $|\Psi\rangle$ and $\langle\tilde{\Psi}|$. More specifically, the CCM employs the exponential parametrizations, $|\Psi\rangle = e^S|\Phi\rangle$ and $\langle\tilde{\Psi}| = \langle\Phi|\tilde{S}e^{-S}$. These states are chosen with a normalization such that $\langle\tilde{\Psi}|\Psi\rangle = 1$ [i.e., with $\langle\tilde{\Psi}| = (\langle\Psi|\Psi\rangle)^{-1}\langle\Psi|$], and with $|\Psi\rangle$ itself satisfying the intermediate normalization condition $\langle\Phi|\Psi\rangle = 1 = \langle\Phi|\Phi\rangle$. The correlation operator S is expressed as $S = \sum_{I \neq 0} \mathcal{S}_I C_I^+$ and its counterpart is $\tilde{S} = 1 + \sum_{I \neq 0} \tilde{\mathcal{S}}_I C_I^-$. The operators $C_I^+ \equiv (C_I^-)^\dagger$, with $C_0^+ \equiv 1$, have the property that $\langle\Phi|C_I^+ = 0 = C_I^-|\Phi\rangle; \forall I \neq 0$. They form a complete set of multi-spin creation operators with respect to the model state $|\Phi\rangle$. The index I is a set-index that stands for the set of lattice sites whose spin projections on the quantization axis are changed with respect to their values in the model state $|\Phi\rangle$. The ket- and bra-state correlation coefficients $(\mathcal{S}_I, \tilde{\mathcal{S}}_I)$ are calculated by requiring the gs energy expectation value $\bar{H} \equiv \langle\tilde{\Psi}|H|\Psi\rangle$ to be a minimum with respect to each of them. This immediately yields the coupled set of equations $\langle\Phi|C_I^- e^{-S} H e^S |\Phi\rangle = 0$ and $\langle\Phi|\tilde{S}(e^{-S} H e^S - E)C_I^+ |\Phi\rangle = 0; \forall I \neq 0$, which we solve in practice for the correlation coefficients $(\mathcal{S}_I, \tilde{\mathcal{S}}_I)$ within specific truncation schemes described below, by making use of parallel computing routines [43].

It is important to note that while the above CCM parametrizations of $|\Psi\rangle$ and $\langle\tilde{\Psi}|$ are not manifestly Hermitian conjugate, they do preserve the important Hellmann-Feynman theorem at *all* levels of approximation (viz., when the complete set of many-particle configurations $\{I\}$ is truncated [3]). Furthermore, the amplitudes $(\mathcal{S}_I, \tilde{\mathcal{S}}_I)$ form canonically conjugate pairs in a time-dependent version of the CCM, in contrast with the pairs $(\mathcal{S}_I, \mathcal{S}_I^*)$ that come from a manifestly Hermitian conjugate representation for $\langle\tilde{\Psi}| = (\langle\Phi|e^{S^\dagger} e^S |\Phi\rangle)^{-1} \langle\Phi|e^{S^\dagger}$, which are *not* canonically conjugate to each other [3].

In order to treat each lattice site on an equal footing we perform a mathematical rotation of the local spin axes

on each lattice site, such that every spin of the model state aligns along its negative z -axis. Henceforth our description of the spins is given wholly in terms of these locally defined spin coordinate frames. In particular, the multi-spin creation operators may be written as $C_I^+ \equiv s_{i_1}^+ s_{i_2}^+ \cdots s_{i_n}^+$, in terms of the locally defined spin-raising operators $s_i^+ \equiv s_i^x + s_i^y$ on lattice sites i . Having solved for the multi-spin cluster correlation coefficients $(\mathcal{S}_I, \tilde{\mathcal{S}}_I)$ as described above, we may then calculate the gs energy E from the relation $E = \langle\Phi|e^{-S} H e^S |\Phi\rangle$, and the average gs on-site magnetization M from the relation $M \equiv -\frac{1}{N} \langle\tilde{\Psi}|\sum_{i=1}^N s_i^z |\Psi\rangle$ which holds in the rotated local spin coordinates. The quantity M is thus the magnetic order parameter, and it is just the usual sublattice (or staggered) magnetization for the case of the Néel state as CCM model state, for example.

Although the CCM formalism is clearly exact if a complete set of multi-spin configurations $\{I\}$ with respect to the model state $|\Phi\rangle$ is included in the calculation of the correlation operators S and \tilde{S} , in practice it is necessary to use systematic approximation schemes to truncate them to some finite subset. In our earlier paper on the $s = \frac{1}{2}$ version of the present model [1], we employed, as in our previous work [4,41,42,44,45], the localized LSUB n scheme in which all possible multi-spin-flip correlations over different locales on the lattice defined by n or fewer contiguous lattice sites are retained.

However, we note that the number of fundamental LUB n configurations for $s = 1$ and $s = \frac{3}{2}$ becomes appreciably higher than for $s = \frac{1}{2}$, since each spin on each site i can now be flipped up to $2s$ times by the spin-raising operator s_i^+ . Thus, for the cases of $s = 1$ and $s = \frac{3}{2}$ it is more practical, but equally systematic, to use the alternative SUB n - m scheme, in which all correlations involving up to n spin flips spanning a range of no more than m adjacent lattice sites are retained [4,40]. We then set $m = n$, and hence employ the so-called SUB n - n scheme. More generally, the LSUB m scheme is thus equivalent to the SUB n - m scheme for $n = 2sm$ for particles of spin s . For $s = \frac{1}{2}$, LSUB $n \equiv$ SUB n - n ; whereas for $s = 1$, LSUB $n \equiv$ SUB $2n$ - n , and for $s = \frac{3}{2}$, LSUB $n =$ SUB $3n$ - n . The numbers of such fundamental configurations (viz., those that are distinct under the symmetries of the Hamiltonian and of the model state $|\Phi\rangle$) that are retained for the Néel and semi-stripped states of the current $s = 1$ and $s = \frac{3}{2}$ models at various SUB n - n levels are shown in Table 1. We note that the distinct configurations given in Table 1 are defined with respect to the Union Jack geometry described in Sec. 2, in which the B sublattice sites of Fig. 1(a) are defined to have four NN sites, and the A sublattice sites are defined to have the eight NN sites joined to them by either J_1 bonds or J_2 bonds. If we chose instead to work in the square-lattice geometry, by contrast, each site would have four NN sites.

Although we never need to perform any finite-size scaling, since all CCM approximations are automatically performed from the outset in the $N \rightarrow \infty$ limit, we do need as a last step to extrapolate to the $n \rightarrow \infty$ limit in the truncation index n . We use the same well-tested scaling

Table 1: Number of fundamental SUB n - n configurations (N_f) for the semi-stripped and canted states of the spin-1 and spin- $\frac{3}{2}$ Union Jack models, based on the Union Jack geometry defined in the text.

Method	$s = 1$		$s = \frac{3}{2}$	
	N_f		N_f	
	semi-stripped	canted	semi-stripped	canted
SUB2-2	3	9	3	9
SUB4-4	115	556	115	618
SUB6-6	7826	52650	9862	68365

laws as for the $s = \frac{1}{2}$ model for the gs energy per spin E/N and the average gs on-site magnetization M ,

$$E/N = a_0 + a_1 n^{-2} + a_2 n^{-4}, \quad (6)$$

$$M = b_0 + b_1 n^{-1} + b_2 n^{-2}. \quad (7)$$

4 Results

We present results of CCM calculations for both the spin-1 and spin- $\frac{3}{2}$ Union Jack models with the Hamiltonian of Eq. (1), for given parameters ($J_1 = 1$, J_2), based respectively on the Néel, canted and semi-stripped states as CCM model states. Our computational power is such that we can perform SUB n - n calculations for each model state with $n \leq 6$.

4.1 Néel state versus the canted state

Results are first presented that are obtained using the Néel and canted model states. While classically we have a second-order phase transition from Néel order (for $\kappa < \kappa_c^{\text{cl}}$) to canted order (for $\kappa > \kappa_c^{\text{cl}}$), where $\kappa \equiv J_2/J_1$, at a value $\kappa_c^{\text{cl}} = 0.5$, using the CCM we find strong indications of a shift of this critical point to a higher value $\kappa_{c1} \approx 0.58$ in the spin-1 case and $\kappa_{c1} \approx 0.545$ in the spin- $\frac{3}{2}$ quantum case as we explain in detail below. These may be compared with the even higher value $\kappa_{c1} \approx 0.66$ found previously [1] for the spin- $\frac{1}{2}$ case.

Thus, just as for the spin- $\frac{1}{2}$ case, curves such as those in Fig. 2 show that the Néel model state ($\phi = 0$) gives the minimum gs energy for all values of $\kappa < \kappa_{c1}$ where $\kappa_{c1} = \kappa_{c1}^{\text{SUB}n-n}$ is also dependent on the level of SUB n - n approximation, as we see clearly in Fig. 3. Conversely, for $\kappa > \kappa_{c1}$ the minimum in the energy is found to occur at a value $\phi \neq 0$. If we consider the canting angle ϕ itself as an order parameter (i.e., $\phi = 0$ for Néel order and $\phi \neq 0$ for canted order) a typical scenario for a first-order phase transition would be the appearance of a two-minimum structure for the gs energy as a function of ϕ . If we therefore admit such a scenario, in the typical case one would expect various special points in the transition region, namely the phase transition point κ_{c1} itself where

the two minima have equal depth, plus one or two instability points κ_{i1} and κ_{i2} where one or other of the minima (at $\phi = 0$ and $\phi \neq 0$ respectively) disappears. By contrast, a second-order phase transition might manifest itself via a one-minimum structure for the gs energy as a function of ϕ , in which the single minimum moves smoothly and continuously from the value $\phi = 0$ for all values of $\kappa < \kappa_{c1}$ to nonzero value $\phi \neq 0$ for $\kappa > \kappa_{c1}$.

Results for the gs energy per spin calculated in the SUB4-4 approximation based on the canted state as the CCM model state are shown in Fig. 2 as a function of the canting angle. Curves such as those shown in Fig. 2 for the SUB4-4 case show that what happens for this model at this level of approximation is that for $\kappa \lesssim 0.592$ for $s = 1$ and for $\kappa \lesssim 0.560$ for $s = \frac{3}{2}$, the only minimum in the gs energy is at $\phi = 0$ (Néel order). As these values are approached from below the SUB4-4 energy curves become extremely flat near $\phi = 0$, indicating the disappearance at $\phi = 0$ of the second derivative $d^2E/d\phi^2$ (and possibly also of one or more of the higher derivatives $d^nE/d\phi^n$ with $n \geq 3$), as well as of the first derivative $dE/d\phi$. Then, for all values $\kappa \gtrsim 0.592$ for $s = 1$ and $\kappa \gtrsim 0.560$ for $s = \frac{3}{2}$, the SUB4-4 curves develop a minimum at a value $\phi \neq 0$ which is also the global minimum. The state for $\phi \neq 0$ is thus the quantum analogue of the classical canted phase. The fact that the antiferromagnetic Néel order survives into the classically unstable regime is another example of the well-known phenomenon that quantum fluctuations tend to promote collinear order in magnetic spin-lattice systems, as has been observed in many other such cases (see e.g., Ref. [41,46]). Thus, this collinear Néel-ordered state survives into a region where classically it becomes unstable with respect to the non-collinear canted state. As expected, as s is increased the value of κ_{c1} decreases towards the classical value 0.5

A detailed inspection of the curves shown in Fig. 3 for various SUB n - n approximation shows that the crossover from one minimum ($\phi = 0$, Néel) solution to the other ($\phi \neq 0$, canted) appears to be continuous for both the $s = 1$ and $s = \frac{3}{2}$ cases indicating a second-order transition according to the above scenario. Thus, based on the evidence presented so far of the gs energies of the Néel and canted phases, it would appear that the transition at $\kappa = \kappa_{c1}$ between these two phases is second-order.

Table 2 shows the critical values $\kappa_{c1}^{\text{SUB}n-n}$ at which the transition between the Néel and canted phases occurs in the various SUB n - n approximations shown in Fig. 3. In the past we have found that a simple linear extrapolation, $\kappa_{c1}^{\text{SUB}n-n} = a_0 + a_1 n^{-1}$, yields a good fit to such critical points. This seems to be the case here too, just as for the spin- $\frac{1}{2}$ case [1]. The corresponding ‘‘SUB ∞ ’’ estimates from the SUB n - n data in Table 2 are $\kappa_{c1} = 0.585 \pm 0.002$ for $s = 1$, and $\kappa_{c1} = 0.557 \pm 0.001$ for $s = \frac{3}{2}$, where the quoted errors are simply a combination of the standard deviations from the fits and of the computational uncertainties associated with the $\kappa_{c1}^{\text{SUB}n-n}$ points themselves. We also present other independent estimates of κ_{c1} below.

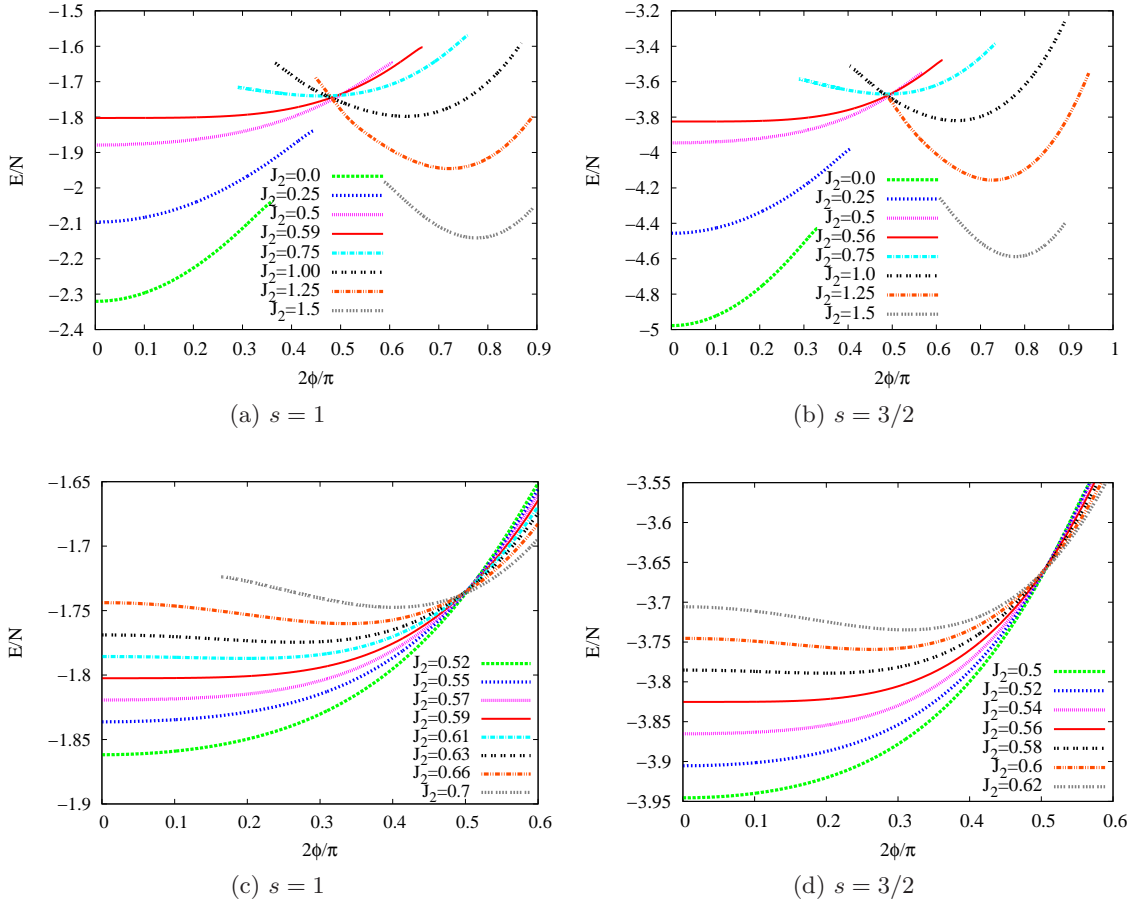


Fig. 2: Ground-state energy per spin of the spin-1 and spin- $\frac{3}{2}$ Union Jack Hamiltonian of Eq. (1) with $J_1 \equiv 1$, using the SUB4-4 approximation of the CCM with the canted model state, versus the canting angle ϕ , for various values of J_2 . For the case of $s = 1$, for $J_2 \lesssim 0.592$ in this approximation the minimum is at $\phi = 0$ (Néel order), whereas for $J_2 \gtrsim 0.592$ the minimum occurs at $\phi = \phi_{\text{SUB4-4}} \neq 0$, indicating a phase transition at $J_2 \approx 0.592$ in this SUB4-4 approximation. For the case of $s = \frac{3}{2}$, for $J_2 \lesssim 0.560$ in this approximation the minimum is at $\phi = 0$ (Néel order), whereas for $J_2 \gtrsim 0.560$ the minimum occurs at $\phi = \phi_{\text{SUB4-4}} \neq 0$, indicating a phase transition at $J_2 \approx 0.560$ in this SUB4-4 approximation.

Figure 2 also displays the feature that for certain values of J_2 with $J_1 \equiv 1$ (or, equivalently, κ) CCM solutions at a given SUB n - n level of approximation (viz., SUB4-4

in Fig. 2) exist only for certain ranges of the canting angle ϕ . For example, for the pure square-lattice HAF ($\kappa = 0$) the CCM SUB4-4 solution based on a canted model state only exists for $0 \leq \phi \lesssim 0.182\pi$ when $s = 1$, and for $0 \leq \phi \lesssim 0.166\pi$ when $s = \frac{3}{2}$. In this case, where the Néel solution is the stable ground state, if we attempt to move too far away from Néel collinearity the CCM equations themselves become “unstable” and simply do not have a real solution. Similarly, we see from Fig. 2 that for $\kappa = 1.5$, for example, the CCM SUB4-4 solution exists only for $0.294\pi \lesssim \phi \leq 0.446\pi$ when $s = 1$ and for $0.302\pi \lesssim \phi \leq 0.446\pi$ when $s = \frac{3}{2}$. In this case the stable ground state is a canted phase, and now if we attempt either to move too close to Néel collinearity or to increase the canting angle too close to its asymptotic value of $\pi/2$, the real solution terminates.

Table 2: The critical value $\kappa_{c_1}^{\text{SUB}n-n}$ at which the transition between the Néel phase ($\phi = 0$) and the canted phase ($\phi \neq 0$) occurs in the SUB n - n approximation using the CCM with (Néel or) canted state as model state.

Method	$s = 1$	$s = \frac{3}{2}$
	$\kappa_{c_1}^{\text{SUB}n-n}$	$\kappa_{c_1}^{\text{SUB}n-n}$
SUB2-2	0.598	0.563
SUB4-4	0.592	0.560
SUB6-6	0.589	0.559
SUB ∞	0.585 ± 0.002	0.557 ± 0.001

Terminations of CCM solutions like those discussed above are very common and have been very well doc-

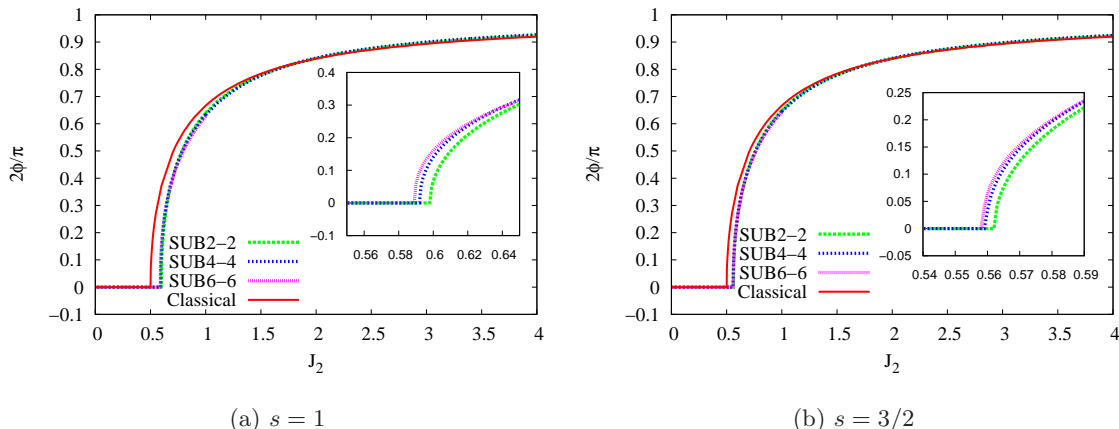


Fig. 3: The angle $\phi_{\text{SUB}n-n}$ that minimizes the energy $E_{\text{SUB}n-n}(\phi)$ of the (a) spin-1 and (b) spin- $\frac{3}{2}$ Union Jack Hamiltonian of Eq. (1) with $J_1 \equiv 1$, in the SUB n - n approximations with $n = \{2, 4, 6\}$, using the canted model state, versus J_2 . The corresponding classical result ϕ_{cl} from Eq. (4) is shown for comparison. We find in the SUB n - n quantum case with $n \geq 2$ a second-order phase transition (e.g., for SUB6-6 at $J_2 \approx 0.589$ for $s = 1$ and $J_2 \approx 0.559$ for $s = \frac{3}{2}$). In the classical case there is a second-order phase transition at $J_2 = 0.5$.

umented [4]. Such termination points always arise due to the solution of the CCM equations becoming complex there. Beyond such points there exist two branches of entirely unphysical complex conjugate solutions [4]. In the region where the solution reflecting the true physical solution is real there actually also exists another (unstable) real solution. However, only the shown branch of these two solutions reflects the true (stable) physical ground state, while the other branch does not. The physical branch is usually easily identified in practice as the one which becomes exact in some known (e.g., perturbative) limit. It then meets the corresponding unphysical branch at some termination point (with infinite slope on Fig. 2), beyond which no real solutions exist. The LSUB n or SUB n - n termination points are themselves also reflections of the quantum phase transitions in the real system, and may be used to estimate the position of the phase boundary [4], although we do not do so for this first critical point since we have more accurate criteria, one of which has already been discussed above. Another will be discussed below.

Before doing so, however, we wish to give some further indication of the accuracy of our results. Thus in Table 3 we show data for the cases of the spin-1 and spin- $\frac{3}{2}$ HAF on the square lattice (corresponding to the case $\kappa = 0$ of the present Union Jack model). We present our CCM results in various SUB n - n approximations (with $2 \leq n \leq 6$) based on the Union Jack geometry using the Néel model state. Results are given for the gs energy per spin E/N , and the magnetic order parameter M , which in this case is simply the staggered magnetization. We also display our extrapolated ($n \rightarrow \infty$) results using the schemes of Eqs. (6) and (7) with the data set $n = \{2, 4, 6\}$. The results are robust, and for comparison purposes we also show for the spin-1 case, the corresponding results using a spin wave theory (SWT) technique [47] and from a linked-cluster series expansion (SE) method [48]. Our

Table 3: Ground-state energy per spin E/N and magnetic order parameter M (i.e., the average on-site magnetization) for the spin-1 and spin- $\frac{3}{2}$ square-lattice HAF. We show CCM results obtained for the Union Jack model with $J_1 = 1$ and $J_2 = 0$ using the Néel model state in various CCM SUB n - n approximations defined on the Union Jack geometry described in Sec. 2. We compare our extrapolated ($n \rightarrow \infty$) results using Eqs. (6) and (7) and our SUB n - n data sets with other calculations.

Method	$s = 1$		$s = \frac{3}{2}$	
	E/N	M	E/N	M
SUB2-2	-2.29504	0.9100	-4.94393	1.4043
SUB4-4	-2.32033	0.8687	-4.97758	1.3618
SUB6-6	-2.32537	0.8488	-4.98352	1.3423
SUB ∞	-2.3295	0.800	-4.9882	1.295
SWT ^a	-2.3282	0.8043		
SE ^b	-2.3279(2)	0.8039(4)		

^a SWT (Spin Wave Theory) for square lattice [47]

^b SE (Series Expansion) for square lattice [48]

own extrapolated results are in good agreement with these results and own previous CCM results [49].

The CCM results for the gs energy per spin are shown in Fig. 4 for various SUB n - n approximations based on the canted (and Néel) model states, with the canting angle $\phi_{\text{SUB}n-n}$ chosen to minimize the energy $E_{\text{SUB}n-n}(\phi)$, as shown in Fig. 3. We also show separately the extrapolated (SUB ∞) results obtained from Eq. (6) using the data set $n = \{2, 4, 6\}$ shown. As is expected from our previous discussion the energy curves themselves show very little evidence of the phase transition at $\kappa = \kappa_{c1}$, with the energy and its first derivative seemingly continuous for both the spin-1 and spin- $\frac{3}{2}$ cases.

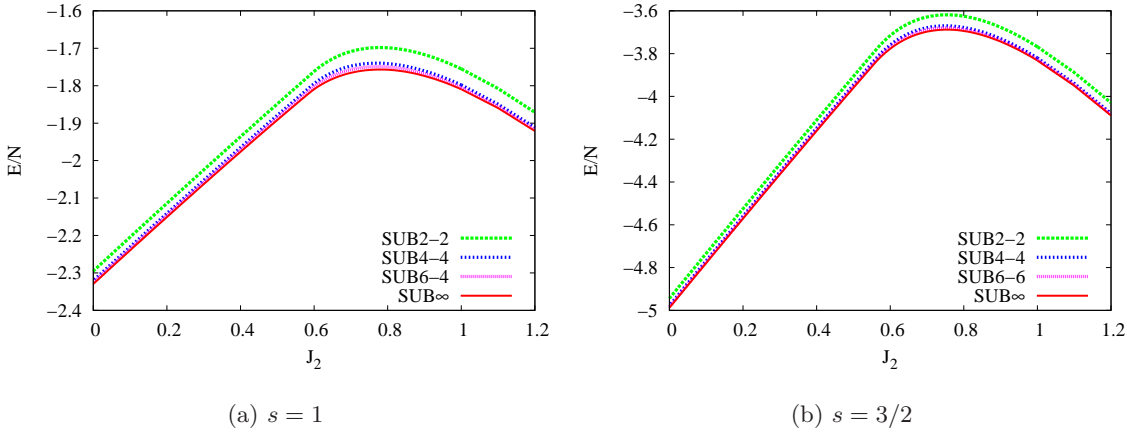


Fig. 4: Ground-state energy per spin versus J_2 for the Néel and canted phases of the (a) spin-1 and (b) spin- $\frac{3}{2}$ Union Jack Hamiltonian of Eq. (1) with $J_1 \equiv 1$. The CCM results using the canted model state are shown for various $\text{SUB}n-n$ approximations with $n = \{2, 4, 6\}$ with the canting angle $\phi = \phi_{\text{LSUB}n}$ that minimizes $E_{\text{SUB}n-n}(\phi)$. We also show the $n \rightarrow \infty$ extrapolated result from using Eq. (6).

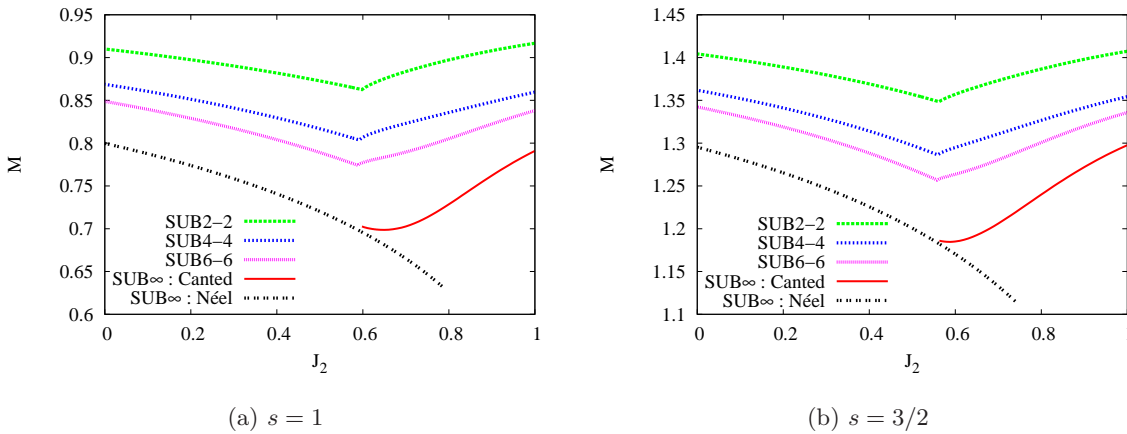


Fig. 5: Ground-state magnetic order parameter (i.e., the average on-site magnetization) versus J_2 for the Néel and canted phases of the (a) spin-1 and (b) spin- $\frac{3}{2}$ Union Jack Hamiltonian of Eq. (1) with $J_1 \equiv 1$. The CCM results using the canted model state are shown for various $\text{SUB}n-n$ approximations with $n = \{2, 4, 6\}$, with the canting angle $\phi = \phi_{\text{SUB}n-n}$ that minimizes $E_{\text{SUB}n-n}(\phi)$. We also show the $n \rightarrow \infty$ extrapolated result from using Eq. (7).

The transition between the Néel and canted phases is observed much more clearly in our corresponding results for the gs magnetic order parameter M (the average on-site magnetization) shown in Fig. 5. For the raw $\text{SUB}n-n$ data we display the results for the Néel phase only for values of $\kappa < \kappa_{c_1}^{\text{SUB}n-n}$ for clarity. However, the extrapolated ($\text{SUB}\infty$) results for the Néel phase are shown for a wider range of values of κ , using the extrapolation scheme of Eq. (7) and the $\text{SUB}n-n$ results based on the Néel model state. For the canted phase (for which $\phi_{\text{SUB}n-n} \neq 0$) we can clearly only show the extrapolated ($\text{SUB}\infty$) results using Eq. (7), for regions of κ for which we have data for all of the set $n = \{2, 4, 6\}$. We see from Table 2 that we are limited (by the $\text{SUB}2-2$ results) to values $\kappa > \kappa_{c_1}^{\text{SUB}2-2} \approx 0.598$ for the $s = 1$ case, and $\kappa > \kappa_{c_1}^{\text{SUB}2-2} \approx 0.563$ for the $s = \frac{3}{2}$ case. From

the data shown in Fig. 5(a) for the case of $s = 1$, simple extrapolations of the $\text{SUB}\infty$ curve to lower values of $\kappa < \kappa_{c_1}^{\text{SUB}2-2} \approx 0.598$ using simple spline fits in κ give a corresponding estimate of $\kappa_{c_1} \approx 0.580 \pm 0.015$ at which the Néel and canted phases meet. The $\text{SUB}n-n$ extrapolations yield a nonzero value for the average on-site magnetization of $M \approx 0.707 \pm 0.003$ at the phase transition point κ_{c_1} . Similarly for the case of $s = \frac{3}{2}$ in Fig. 5(b), simple extrapolations of the $\text{SUB}\infty$ curve to lower values of $\kappa < \kappa_{c_1}^{\text{SUB}2-2} \approx 0.563$ using simple spline fits in κ give a corresponding estimate of $\kappa_{c_1} \approx 0.535 \pm 0.005$ at which the Néel and canted phases meet. The $\text{SUB}n-n$ extrapolations yield a nonzero value for the average on-site magnetization of $M \approx 1.192 \pm 0.002$ at the phase transition point κ_{c_1} . Thus the evidence from the behaviour of the order parameter is that the transition at κ_{c_1} is a first-order one

for both the cases $s = 1$ and $s = \frac{3}{2}$, in the sense that the order parameter does not go to zero at κ_{c_1} , although it is certainly continuous at this point. The extrapolated curves also provide every indication that the derivative of the order parameter as a function of κ is also continuous (or very nearly so) at $\kappa = \kappa_{c_1}$ for both the cases $s = 1$ and $s = \frac{3}{2}$.

In Fig. 6 we also show the corresponding extrapolated (SUB ∞) results for the average on-site magnetization as a function of J_2 (with $J_1 \equiv 1$), or hence equivalently as a function of κ , for both the A sites (M_A) and the B sites (M_B) of the Union Jack lattice. We recall that, as shown in Fig. 1, each of the A and B sites is connected to four NN sites on the square lattice by J_1 bonds, whereas each of the A sites is additionally connected to four NNN sites on the square lattice by J_2 bonds. The extrapolations are shown in exactly the same regions, and for the same reasons, as those shown in Fig. 5.

We also comment briefly on the large- J_2 behaviour of our results for the canted phase. (We note that for computational purposes it is easier to re-scale the original Hamiltonian of Eq. (1) by putting $J_2 \equiv 1$ and considering small values of J_1 .) For the case of $s = \frac{1}{2}$ which we studied previously [1], the most interesting feature of the CCM results using the canted state as model state is that in all LSUB n approximations with $n > 2$ a termination point $\kappa_t^{\text{LSUB}n}$ is reached, beyond which no real solution can be found. For example, we found [1] the values $\kappa_t^{\text{LSUB}4} \approx 80$ and $\kappa_t^{\text{LSUB}6} \approx 80$. This is a first indication that the canted state becomes unstable at very large values of κ against the formation of another (as yet unknown) state, as we discuss further in Sec. 4.2 below. By contrast, in the present cases of $s = 1$ and $s = \frac{3}{2}$, the canted state shows no sign of any instability for any SUB n - n approximation with $n = \{2, 4, 6\}$ for all values of $\kappa \leq 100$ studied.

Simple extrapolations to the $\kappa \rightarrow \infty$ limit of the gs energy using the data at $\kappa \leq 100$ show that at large J_2 values we have $E/N \rightarrow -1.1652J_2$ for $s = 1$ and $E/N \rightarrow -2.4943J_2$ for $s = \frac{3}{2}$. These numerical coefficients are almost exactly half of the values quoted in Table 3 for the case $J_2 = 0$. This is as expected since both the $\kappa \rightarrow 0$ and the $\kappa \rightarrow \infty$ limits of the Union Jack model are the square-lattice HAF, where in the latter case the square lattice contains only half the original sites, namely the A sites. Similarly, the extrapolated SUB ∞ values at larger values of $\kappa = 100$ for the on-site magnetization on the A sites are $M_A \rightarrow 0.807$ for $s = 1$ and $M_A \rightarrow 1.303$ for $s = \frac{3}{2}$. These values are again in very good agreement with those shown in Table 3 for the $J_2 = 0$ limit. The corresponding asymptotic values for the B-site magnetization are consistent with $M_B \rightarrow 1.0$ and $M_B \rightarrow 1.5$, as expected for large values of J_2 .

4.2 Canted state versus the semi-stripped state

For the Union Jack model considered here, but for the case $s = \frac{1}{2}$ studied previously, we predicted [1] a second phase transition at $\kappa = \kappa_{c_2} \approx 125 \pm 5$ using the same CCM technique as used here. At this upper transition the ferrimagnetic

quantum canted phase shown in Fig. 1(a) gives way to the quantum ferrimagnetic semi-stripped phase shown in Fig. 1(b), such that for value $\kappa > \kappa_{c_2}$ the semi-stripped phase becomes lower in energy. In order to investigate the possible similar stabilization of the quantum semi-stripped state at high values of the frustration parameter κ , we have performed similar CCM calculations here, for the $s = 1$ and $s = \frac{3}{2}$ cases, based on the semi-stripped state as model state.

As already noted above, we find no sign of instability in the canted state, for either of the cases $s = 1$ or $s = \frac{3}{2}$, for any level of SUB n - n approximation with $n \leq 6$ at all values $\kappa \leq 100$ investigated, unlike for the corresponding LSUB n approximations in the $s = \frac{1}{2}$ case that terminated in this range for all values $2 < n \leq 6$ investigated. Furthermore, we find no evidence at all that the semi-stripped phase has lower energy than the canted phase for any value of κ for either of the case $s = 1$ or $s = \frac{3}{2}$. Nonetheless, simple extrapolations to the $\kappa \rightarrow \infty$ limit of the gs energy of the semi-stripped phase, using the SUB n - n data with $n = \{2, 4, 6\}$ at $\kappa \leq 1000$, show that at large J_2 values we have $E/N \rightarrow -1.1646J_2$ for $s = 1$ and $E/N \rightarrow -2.4939J_2$ for $s = \frac{3}{2}$ (with $J_1 \equiv 1$). The corresponding asymptotic ($\kappa \rightarrow \infty$) values for the average gs on-site magnetization of the semi-stripped state are $M_A \rightarrow 0.807$ on the A sites and $M_B \rightarrow 1.303$ on the A sites and $M_B \rightarrow 1.5$ on the B sites for the $s = \frac{3}{2}$ case, just as for the corresponding large- κ limits of the canted state, and as corresponds to the pure square-lattice HAF as already noted above.

5 Discussion and conclusions

In an earlier paper [1] we used the CCM to study the effect of quantum fluctuations on the zero-temperature gs phase diagram of a frustrated spin- $\frac{1}{2}$ Heisenberg antiferromagnet (HAF) defined on the 2D Union Jack lattice of Fig. 1. In the present paper we have extended the analysis to the two computationally more challenging cases where all the lattice spins have spin quantum number either $s = 1$ or $s = \frac{3}{2}$. We have once again concentrated on the case where the NN J_1 bonds are antiferromagnetic ($J_1 > 0$) and the competing NNN $J_2 \equiv \kappa J_1$ bonds in the Union Jack array have a strength in the range $0 \leq \kappa < \infty$. On the underlying bipartite square lattice there are thus two types of sites, viz., the A sites that are connected to the four NN sites on the B sublattice with J_1 bonds and to the four NNN sites on the A sublattice with J_2 bonds, and the B sites that are connected only to the four NN sites on the A sublattice with J_1 bonds. The $\kappa = 0$ limit of the model thus corresponds to the HAF on the original square lattice (of both A and B sites), while the $\kappa \rightarrow \infty$ limit corresponds to the HAF on the square lattice comprised of only A sites. We have seen that at the classical level (corresponding to the case where the spin quantum number $s \rightarrow \infty$) this Union Jack model has only two stable gs phases, one with Néel order for $\kappa < \kappa_c^{\text{cl}} = 0.5$ and another with canted ferrimagnetic order for $\kappa > \kappa_c^{\text{cl}}$. We have therefore first used these two classical states as

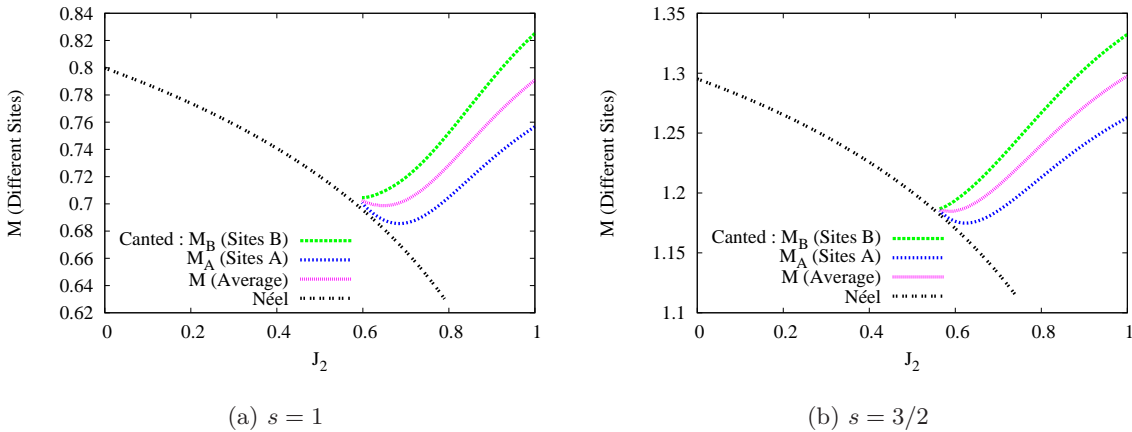


Fig. 6: Extrapolated curves (SUB ∞) for the ground-state magnetic order parameters (i.e., the on-site magnetizations) M_A at sites A (joined by eight bonds to other sites) and M_B at sites B (joined by four bonds to other sites) of the Union Jack lattice [and see Fig. 1(a)] versus J_2 for the Néel and canted phases of the (a) spin-1 and (b) spin- $\frac{3}{2}$ Union Jack Hamiltonian of Eq. (1) with $J_1 \equiv 1$. The CCM results using the canted model state are shown for various SUB n - n approximations ($n = \{2, 4, 6\}$) with the canting angle $\phi = \phi_{\text{SUB}n-n}$ that minimizes $E_{\text{SUB}n-n}(\phi)$.

CCM model states to investigate the effects of quantum fluctuations on them.

For the spin-1 model we find that the phase transition between the Néel antiferromagnetic phase and the canted ferrimagnetic phase occurs at the value $\kappa_{c_1} = 0.580 \pm 0.015$, whereas for the spin- $\frac{3}{2}$ model we find that the phase transition occurs at $\kappa_{c_1} = 0.545 \pm 0.015$. The evidence from our calculations is that the transition at κ_{c_1} is a subtle one. From the energies of the two phases it appears that the transition is second-order, as in the classical case. However, on neither side of the transition at κ_{c_1} does the order parameter M (i.e., the average on-site magnetization) go to zero. Instead, as $\kappa \rightarrow \kappa_{c_1}$ from either side, $M \rightarrow 0.707 \pm 0.003$ for the $s = 1$ case and $M \rightarrow 1.192 \pm 0.002$ for the $s = \frac{3}{2}$ case, which are more indicative of a first-order transition. Furthermore, the slope $dM/d\kappa$ of the average on-site magnetization as a function of κ also seems to be either continuous or to have only a very weak discontinuity at $\kappa = \kappa_{c_1}$ in both of the cases $s = 1$ and $s = \frac{3}{2}$.

In the case of the previously studied spin- $\frac{1}{2}$ model [1] we found evidence for a second quantum phase transition at a value $\kappa = \kappa_{c_2} \approx 125 \pm 5$ at which the quantum ferrimagnetic canted phase for $\kappa < \kappa_{c_2}$ yields to a lower-energy quantum ferrimagnetic semi-stripped phase for $\kappa > \kappa_{c_2}$. Our LSUB n results with $n > 2$ for the spin- $\frac{1}{2}$ model gave clear evidence that the canted phase terminated at some value $\kappa_t^{\text{LSUB}n}$ such that for $\kappa > \kappa_t^{\text{LSUB}n}$ no real solution based on the canted state as model state existed. These termination points were a preliminary signal of the actual phase transition at κ_{c_2} . In neither the $s = 1$ nor $s = \frac{3}{2}$ cases considered here do we find any corresponding upper termination points for any SUB n - n approximation based on the canted state as model state, for any value of $n \leq 6$ and for any value of κ up to the highest value $\kappa = 100$ investigated. Furthermore, for all approximation and for all values of κ investigated the semi-stripped phase always

lies higher in energy than the quantum canted phase for both the $s = 1$ and $s = \frac{3}{2}$ cases, unlike what was found [1] for the $s = \frac{1}{2}$ case. Thus, our results clearly show that only the $s = \frac{1}{2}$ model has a second quantum phase transition at $\kappa = \kappa_{c_2}$ between the two ferrimagnetic (canted and semi-stripped) phases. No such transition is predicted to occur at a finite value of κ for either of the $s = 1$ or $s = \frac{3}{2}$ cases.

To the best of knowledge no other studies of the Union Jack model for lattice spins with spin quantum number $s > \frac{1}{2}$ have been performed, and hence we have no other results with which to compare. Nevertheless, the consistency of the present results and those of our previously studied spin- $\frac{1}{2}$ case [1] give credence to our results. Furthermore, as has been noted elsewhere [7], high-order CCM results of the sort presented here have been seen to provide very accurate and reliable results for a wide range of such highly frustrated spin-lattice models. Many previous applications of the CCM to unfrustrated spin models have given excellent quantitative agreement with other numerical methods (including exact diagonalization (ED) of small lattices, quantum Monte Carlo (QMC), and series expansion (SE) techniques). A typical example is the HAF on the square lattice, which is the $\kappa = 0$ limit of the present model [1]. We have compared our own results for this $\kappa = 0$ case with both SWT and SE results, both for the spin- $\frac{1}{2}$ case in our earlier work [1] and for the spin-1 case here, and shown that there is excellent agreement in both cases. This adds further credence to the validity of our results at nonzero values of κ .

Acknowledgment

We thank D.J.J. Farnell for fruitful discussions.

References

1. R.F. Bishop, P.H.Y. Li, D.J.J. Farnell, C.E. Campbell, Phys. Rev. B **82**, 024416 (2010)
2. R.F. Bishop, Theor. Chim. Acta **80** 95 (1991)
3. R.F. Bishop, in *Microscopic Quantum Many-Body Theories and Their Applications*, Lecture Notes in Physics **510**, J Navarro, A Polls (eds.), (Springer, Berlin, 1998), p. 1
4. D.J.J. Farnell, R.F. Bishop, in *Quantum Magnetism*, Lecture Notes in Physics **645**, U. Schollwöck, J. Richter, D.J.J. Farnell, R.F. Bishop (eds.), (Springer, Berlin, 2004), p. 307
5. R. Darradi, J. Richter, S.E. Krüger, J. Phys.: Condens. Matter **16** 2681 (2004)
6. R.F. Bishop, P.H.Y. Li, R. Darradi, J. Schulenburg, J. Richter, Phys. Rev. B **78**, 054412 (2008)
7. R.F. Bishop, P.H.Y. Li, R. Darradi, J. Richter, J. Phys.: Condens. Matter **20**, 255251 (2008)
8. R. Darradi, J. Richter, D.J.J. Farnell, J. Phys.: Condens. Matter **17** 341 (2005)
9. U. Schollwöck, J. Richter, D.J.J. Farnell, R.F. Bishop (eds.), *Quantum Magnetism*, Lecture Notes in Physics **645** (Springer, Berlin, 2004)
10. G. Misguich, C. Lhuillier, in *Frustrated Spin Systems*, H. T. Diep (ed.), (World Scientific, Singapore, 2005), p. 229
11. J.B. Parkinson, D.J.J. Farnell, *An Introduction to Quantum Spin Systems*, Lecture Notes in Physics **816** (Springer, Berlin, 2010)
12. E. Manousakis, Rev. Mod. Phys. **63**, 1 (1991)
13. A.W. Sandvik, Phys. Rev. B **56**, 11678 (1997)
14. R.F. Bishop, D.J.J. Farnell, J.B. Parkinson, Phys. Rev. B **58**, 6394 (1998)
15. R. Darradi, J. Richter, J. Schulenburg, R.F. Bishop, P.H.Y. Li, J. Phys.: Conf. Ser. **145**, 012049 (2009)
16. R. Darradi, O. Derzhko, R. Zinke, J. Schulenburg, S. E. Krüger, J. Richter, Phys. Rev. B **78**, 214415 (2008)
17. J. Oitmaa, Zheng Weihong, Phys. Rev. B **54**, 3022 (1996)
18. R.R.P. Singh, Zheng Weihong, C. J. Hamer, J. Oitmaa, Phys. Rev. B **60**, 7278 (1999)
19. V. N. Kotov, J. Oitmaa, O. Sushkov, Zheng Weihong, Phil. Mag. B **80**, 1483 (2000)
20. J. Sirker, Zheng Weihong, O.P. Sushkov, J. Oitmaa, Phys. Rev. B **73**, 184420 (2006)
21. T. Pardini, R.R.P. Singh, Phys. Rev. B **79**, 094413 (2009)
22. E. Dagotto, A. Moreo, Phys. Rev. Lett. **63**, 2148 (1989); Phys. Rev. B **39** 4744(R) (1989)
23. H.J. Schulz, T.A.L. Ziman, Europhys. Lett. **18**, 355 (1992); H.J. Schulz, T.A.L. Ziman, D. Poilblanc, J. Phys. I **6**, 675 (1996)
24. J. Richter, J. Schulenburg, Eur. Phys. J. B **73**, 117 (2010)
25. L. Isaev, G. Ortiz, J. Dukelsky, Phys. Rev. B **79**, 024409 (2009)
26. B.S. Shastry, B. Sutherland, Physica B **108**, 1069 (1981)
27. R. Darradi, J. Richter, D.J.J. Farnell, Phys. Rev. B **72**, 104425 (2005)
28. D.J.J. Farnell, J. Richter, R. Zinke, R.F. Bishop, J. Stat. Phys. **135**, 175 (2009)
29. R.F. Bishop, P.H.Y. Li, D.J.J. Farnell, C.E. Campbell, Phys. Rev. B **79**, 174405 (2009)
30. A. Collins, J. McEvoy, D. Robinson, C. J. Hamer, Zheng Weihong, Phys. Rev. B **73**, 024407 (2006); *ibid.* **75**, 189902(E) (2007)
31. A. Collins, J. McEvoy, D. Robinson, C. J. Hamer, Z. Weihong, J. Phys.: Conf. Ser. **42**, 71 (2006)
32. Weihong Zheng, J. Oitmaa, and C. J. Hamer, Phys. Rev. B **75**, 184418 (2007); *ibid.* **76**, 189903(E) (2007)
33. L. Balents, Nature **464**, 199 (2010)
34. F.D.M. Haldane Phys. Lett. A **93** 464 (1983); Phys. Rev. Lett. **50** 1153 (1983)
35. R.F. Bishop, P.H.Y. Li, R. Darradi, J. Richter, C.E. Campbell, J. Phys.: Condens. Matter **20** 415213 (2008)
36. Y. Kamihara, T. Watanabe, M. Hirano, H. Hosono, J. Am. Chem. Soc. **130** 3296 (2008)
37. F. Ma, Z-Y. Lu, T. Xiang, Phys. Rev. B **78**, 224517 (2008)
38. Q. Si, E. Abrahams, Phys. Rev. Lett. **101**, 076401 (2008)
39. J. Villain, J. Phys. (France) **38**, 385 (1977); J. Villain, R. Bidaux, J. P. Carton, and R. Conte, *ibid.* **41**, 1263 (1980)
40. D.J.J. Farnell, R.F. Bishop, K.A. Gernoth, Phys. Rev. B **63**, 220402(R) (2001)
41. S.E. Krüger, J. Richter, J. Schulenburg, D.J.J. Farnell, R.F. Bishop, Phys. Rev. B **61**, 14607 (2000)
42. D. Schmalfuß, R. Darradi, J. Richter, J. Schulenburg, D. Ihle, Phys. Rev. Lett. **97**, 157201 (2006)
43. We use the program package “Crystallographic Coupled Cluster Method” (CCCM) of D.J.J. Farnell and J. Schulenburg, see <http://www-e.uni-magdeburg.de/jschulen/ccm/index.html>
44. C. Zeng, D.J.J. Farnell, R.F. Bishop, J. Stat. Phys. **90**, 327 (1998)
45. D.J.J. Farnell, R.F. Bishop, K.A. Gernoth, J. Stat. Phys. **108**, 314 (2002)
46. H. Kontani, M. E. Zhitomirsky, K. Ueda, J. Phys. Soc. Jpn. **65**, 1566 (1996)
47. C.J. Hamer, Zheng Weihong, P. Arndt, Phys. Rev. B **46**, 6276 (1992)
48. Zheng Weihong, J. Oitmaa, C.J. Hamer, Phys. Rev. B **43**, 8321 (1991)
49. D.J.J. Farnell, K.A. Gernoth, R.F. Bishop, Phys. Rev. B **64**, 172409 (2001)